Construction and Building Materials 269 (2021) 121253

Contents lists available at ScienceDirect

Construction and Building Materials

journal homepage: www.elsevier.com/locate/conbuildmat

Calculating moisture emissivity of timber members with different surface treatment

Zhongwen Zhang, Zhili He, Zhao-Dong Xu *, Li-Wei Chen

Key Laboratory of Concrete and Prestressed Concrete Structures of Ministry of Education, School of Civil Engineering, Southeast University, Nanjing 210000, PR China

HIGHLIGHTS

- Proposes a method to derive surface moisture emissivity in unsteady transfer process.
- The proposed method only requires overall weight of the sample.
- Moisture emissivity was presented for timber surface with different types of coating.

ARTICLE INFO

Article history:
Received 5 December 2019
Received in revised form 27 September 2020
Accepted 5 October 2020
Available online 23 October 2020

Keywords:
Timber structures
Moisture transfer
Wood painting
Bayesian updating

ABSTRACT

Mechanical property and durability of timber members is significantly affected by their surface moisture emissivity which determines the rate they exchange the moisture with the surrounding air. The surface moisture emissivity depends on various parameters including the air flow rate, the temperature and the surface treatment. However, there currently lacks a suitable method for measuring it in the actual working environment of the timber structures. This paper proposes such a method which can identify the surface moisture emissivity factor for timber members with different kinds of surface treatment in their unsteady moisture transfer process. The method is based on Bayesian updating of the numerical model of moisture transfer process of the wood based on the overall weight change. The numerical model considers coupled transfer of the vapour and the bound water. Influences of the sorption hysteresis were also included. Using the method, moisture emissivity factor of different kinds of timber surfaces can be measured by weighting their small-sized samples exposed to ambient climate. Steady moisture transfer process, controlled temperature and RH environment, or the information of the moisture gradient in the samples are not required. Using the method, surface moisture emissivity factor of a pine wood was determined without and with different kinds of surface paint. The measured factor was validated by additional experimental data.

1. Introduction

Engineering timber products including cross-laminated timber (CLT) and glulam are being increasingly used in the modern building industry. Durability and mechanical property of these timber products are significantly affected by their moisture content. Dimension, stiffness and strength of wood distinctly varies at different moisture content levels, which can introduce eigenstresses and cracks [1–4]. Mechano-Sorptive creep is expected for wood sustaining long-term load with repeated moisture content variations [5]. This kind of creep often dominates the long-term deflection of timber structures [6]. Moreover, wood with a moisture content larger than 20% is vulnerable to fungi, which leads to severe deterioration of its mechanical performances [7–9]. As a hygroscopic material, wood absorbs and desorbs the moisture from the surrounding air. When exposed to a constant relative humidity (RH) and temperature, timber structures eventually reach a constant moisture content known as the equilibrium moisture content. In the working environment of timber structures, on the other hand, the equilibrium is seldom reached. The wood keeps constantly taking and giving away moisture and heat due to the varying RH level and temperature. Gradient and variations of the moisture content and temperature therefore exist in timber structures. Depending on the maximum RH a timber member is exposed, its maximum moisture content and their duration, Eurocode 5 [6] divides the working environment of timber structure to 3 service classes. The design strength and long-term stiffness of a timber members are influenced significantly by its service class [6].

* Corresponding author.
E-mail address: xuzhdgyq@seu.edu.cn (Z.-D. Xu).

https://doi.org/10.1016/j.conbuildmat.2020.121253
0950-0618/

Influenced by the climate, average RH and temperature of the working environment of wood varies significantly in different months of the year [1,10–14]. They also tend to vary daily with the highest RH and lowest temperature often observed in the evening, while the lowest RH and highest temperature observed with the daylight. The surface moisture emissivity of the timber structure is an important property which controls the rate of moisture exchange of the timber member with the surrounding air. Together with dimension of the member, frequency of the RH variation and the conductivity of the moisture in wood, the property determines the moisture variation and gradient in different part of the wood [15,16]. Fragiacomo et al. [17] found that when surface coating is used which increases the surface resistance, eigenstress of the wood in different climates typically reduces. Fortino et al. [18], Gereke and Niemz [15] and Angst and Malo [19] made similar observation. The surface moisture flux is also crucial in crack control in the drying of the green wood [20,21].

The research community has long recognized influences of the surface moisture flux and the corresponding emissivity factor on performance of timber structures. Various research investigations were made. [17,22,23] Siau and Avramidis [24] investigates the surface emissivity factor of wood and concluded that the factor is related both the internal and external moisture resistance and is the affected by fluid characteristics of air and surface condition of the wood. Value of the emissivity factor was calculated based on sorption tests and theoretical solution of their governing differential equation. Liu and Simpson [25], Koc and Houška [26] used inverse identification method to calculate the surface emissivity factor based on optimization of the numerical model of its moisture transfer, which allows to derive the emissivity factor for processes with nonlinear diffusivity factors. Yeo and Smith [27] used the boundary layer theory of the air flow for calculating the surface emissivity factor and validated the results by experimental data regarding drying and sorption of different species of wood. These research investigations, however, assumed a single Fickian process for the moisture transfer and relate the surface flux with total moisture content. The assumption makes no distinction between the bound water and vapour concentration which is unreasonable as the surface moisture flux mainly takes the form of vapour transfer. [28] The calculated factor was therefore often found to be affected by the sorption rate and frequency of the environmental RH variations. [29] For the multi-Fickian models which are physically more accurate, the surface emissivity factors in terms of the vapour flux and vapour concentration (or partial pressure) currently used by researchers are typically estimated and lack experimental validation [13,17,30]. This is complicated by the fact that the moisture emissivity factor is related with complicated parameters associated with individual test such as the air flow rate, surface condition of the timber as well as penetration and quality of the surface painting [24,25,27].

There has been significant advancement in recent years in numerical model of the moisture transfer process in the wood. Krabbenhøft [28], Krabbenhøft and Damkilde [31] proposes to model moisture transfer in wood as two Fickian processes with individual vapour and bound water transfer. Coupling these two processes is a sorption term representing transfer between vapour and the bound water. Frandsen et al. [32] proposes method to consider the hysteresis effect in the sorption curve and equations to calculate explicitly the sorption rate with consideration of the differences between adsorption and desorption at different bound water concentrations. Eitelberger et al. [33] considers microstructure of the wood and uses a method for evaporation rate of the bound water based on local equilibrium of the cell wall and lumen. These models can simulate the unsteady state moisture transfer process with good accuracy. Additional heat transfer process which governs the sorption balance and rate was considered in the model proposed by Fortino et al. [13], Fortino et al. [18] and Eitelberger et al. [33]. However, calculating the surface emissivity can still be difficult even with these models. This is partially due to the fact that the moisture transfer involves significant nonlinearity [34]. Explicit solution for the governing differential equations is not available, and the inverse problem is often ill-posed. In these cases, the Bayesian method is a robust method [35,36].

This paper proposes a method for determining the surface emissivity of timber members. The method uses the Bayesian method to update of the finite element (FE) models from the overall weight measurement of the samples. Controlled environment, sealed cup or detailed measurement of the moisture content of the wood in different layers are not required which makes the method very suitable for field measurement of the surface moisture emissivity of timber structure working in different conditions. Using the proposed method, surface moisture emissivity was measured for neat and different kinds of coated timber surfaces.

2. Methodology

Accurate evaluation of the moisture related mechanical property of timber members requires accurate identification of the surface emissivity factor at the working environment of the timber structures. In these environments, the steady state moisture transfer is seldom reached, and the only easily assessable data would be the overall weight of the sample without advanced equipment [37,38]. This paper investigates using the changes of overall weight of the timber samples to calculate surface emissivity factor of the wood with the Bayesian model updating technique.

2.1. Governing equations for moisture transfer in wood

Moisture content in timber member varies with RH and temperature in surrounding air due to the porous and hydrophilic nature of wood. Modelling variation and gradient of the moisture content in wood is therefore crucial in evaluating eigenstress and mechano-sorptive behaviour of timber structures. Previously, researchers often use a simple Fickian process to describe the moisture transfer. The method, however, does not consider the sorption process and often fails to describe the unsteady moisture transfer. Researchers generally found that explicit consideration of the individual transport of vapour and bound water are required to accurately model the unsteady moisture transfer. [28] These transport processes are coupled by a sorption term which represents evaporation and condensation between bound water and vapour. [32] Sometimes, the heat transfer process is also included in the governing equations which is related with the temperature profile in the wood and therefore related with the equilibrium between bound water and vapour and the sorption rate. [13,18,33] A typical governing equation for the moisture transfer is therefore written as [33]:

$$\frac{\partial c_v}{\partial t} + \frac{\partial}{\partial x} J_v + \dot{c} \frac{f_{cwm}}{f_{lum}} = 0$$

$$\frac{\partial c_b}{\partial t} + \frac{\partial}{\partial x} J_b - \dot{c} = 0$$

$$\frac{\partial \rho h}{\partial t} + \frac{\partial}{\partial x} f + \frac{\partial}{\partial x} J_b h_b f_{cwm} + \frac{\partial}{\partial x} J_v h_v f_{lum} + \dot{c}(h_v - h_b) f_{cwm} = 0 \quad (1)$$

In the equation, c_v is the mass concentration of the water vapour in lumen; c_b is concentration of the bound water in cell wall; T is the temperature; ρ is dry density of the wood; h is heat capacity of the dry wood; t is the time; x is the spatial coordinate; J_b is the effective bound water flux; J_v is the water vapour flux; f is the heat flux; h_b and h_v are the specific enthalpies of bound water and water vapour; f_{cwm} and f_{lum} are the volumetric fraction of the lumens and the cell walls.

Water vapour main exists in lumens of the wood in conjunction with air. Its transport in the wood involves complicated chemical and physical processes. Diffusion due to concentration gradient occurs in the lumen and through pores and pits across lumens following Fick's law. On the other hand, vapour gradient in different lumens causes localized condensation on one side of the cell wall and evaporation on the other side. It was indicated that this kind of transport process actually dominates the overall transport of vapour in wood. [39] At higher temperature, there are also indications that convection process could be significant due to gas pressure differences. However, at the normal temperature range, it was generally agreed by researchers that the vapour transfer in wood can be described by a differential equation shown in Eq. (2) by the gradient law. [28] However, the effective diffusivity is highly nonlinear and significantly varies in different directions in the wood.

$$\boldsymbol{J_v} = -\boldsymbol{D_v}\frac{\partial c_v}{\partial \boldsymbol{X}} \tag{2}$$

In the equation, $\boldsymbol{D_v}$ is the effective diffusivity matrix of the vapour to different directions and J_b is the effective bound water flux.$\boldsymbol{X}$is the spatial coordinate vector.

Transport of the bound water can also be expressed in the similar form shown in Eq. (3) driven by concentration gradient. In the equation, $\boldsymbol{D_b}$ is the diffusivity matrix of the bound water. Particularly, the bonding energy between bound water molecules and the hydroxide group in cell walls varies with the bound water content. Nonlinearity is therefore also expected in the differential equation.

$$\boldsymbol{J_b} = -\boldsymbol{D_b}\frac{\partial c_b}{\partial \boldsymbol{X}} \tag{3}$$

Coupling the vapour and bound water transfer are the sorption term, $\dot{c}$, which represents rate of the phase change between the bound water and water vapour. The sorption rate is related with differences between the current bound water concentration and the equilibrium bound water concentration. Different forms of relations were assumed by different researchers. The most commonly used equation for calculating the sorption rate is probably the model proposed by Frandsen et al. [32]. The method considers explicitly the difference in adsorption and desorption as well as the dramatic reduction of the sorption rate when moisture content approaches the equilibrium value. Detailed parameters of the model were calibrated by the sorption tests [40]. Eitelberger et al. [33] assumes a local equilibrium in calculating the sorption rate between inner surface of the lumen and the air in the lumen. Therefore, the sorption rate is related with average size of the cell walls of the wood and the bound water diffusivity in the microscale. Essentially, an approximately linear relation was adopted between the sorption rate and the equilibrium moisture content differences.

The equilibrium bound water concentration, on the other hand, relates with concentration of the water vapour by the sorption curve. Significant hysteresis effect often exists in sorption curve of wood which indicates that equilibrium moisture content of the wood is not only with the current relative humidity but also with the previous relative humidity history. Various models were proposed by different researchers including the work conducted by Frandsen et al. [32], Patera et al. [41], Peralta [42] and Pedersen [43].

In addition to the transfer process in the wood, the exchanges of the moisture and heat of the wood with the surrounding air controls the moisture content in the wood as the boundary condition. For timber structures in their typical using condition, the exchange of moisture mainly takes the form of vapour flux while the exchange of bound water is often assumed to be zero (that is, assuming enough isolation is provided between the timber member and the ground). At surface of the timber member, a boundary layer exists which has often different vapour concentration with the ambient air due to the vapour exchange. The airflow in the boundary layer can therefore influence the surface emissivity of the timber structure which can be in the laminar or turbulent form depending on its velocity and the surface roughness. In addition, the cutting method and coating often leads to closure of the micropores in the wood which could also influence the vapour exchange mechanism significantly. Instead of modelling these complicated processes, researchers often use a simple surface emissivity factor to characterize surface flux of the wood, as:

$$J_{sv} = k_v(c_{v\_air} - c_v) \text{ for flux of the water vapour}$$

$$J_{sT} = k_T(T_{air} - T_v) \text{ for flux of the heat} \tag{4}$$

In which k_T and k_v are the surface emission factor for transfer of the heat and moisture, respectively, and J_{sT} and J_{sv} are the surface flux of the heat and moisture, respectively.

Finite element discretization and numerical methods

The governing equations presented in Eq. (1) are often solved by the finite element approach. Using Galerkin formulation and backward Euler integration scheme, Eq. (1) can be expressed in the weak form as:

$$\frac{1}{\Delta t}\int N(c_{b,t+\Delta t} - c_{b,t})dV + \int \frac{\delta N}{\delta \boldsymbol{X}}\boldsymbol{D}_b\frac{\delta c_b}{\delta \boldsymbol{X}}dV - \int N\dot{c}dV = 0 \tag{5}$$

$$\frac{1}{\Delta t}\int N(c_{v,t+\Delta t} - c_{v,t})dV + \int \frac{\delta N}{\delta \boldsymbol{X}}\boldsymbol{D_v}\frac{\delta c_v}{\delta \boldsymbol{X}}dV + \int N\dot{c}\frac{f_{cwm}}{f_{lum}}dV = 0 \tag{6}$$

$$\begin{aligned}&\frac{1}{\Delta t}\int N[(\rho u)_{b,t+\Delta t} - (\rho u)_{b,t}]dV + \int \frac{\delta N}{\delta \boldsymbol{X}}\boldsymbol{K}\frac{\delta T}{\delta \boldsymbol{X}}dV\\ &-\int h_{bv}N\dot{c}f_{cwm}dV + \int h_b\frac{\delta N}{\delta \boldsymbol{X}}\boldsymbol{D_b}\frac{\delta c_b}{\delta \boldsymbol{X}}f_{cwm}dV\\ &+\int h_v\frac{\delta N}{\delta \boldsymbol{X}}\boldsymbol{D_b}\frac{\delta c_v}{\delta \boldsymbol{X}}f_{lum}dV = 0\end{aligned} \tag{7}$$

In the equation, V is the arbitrary volume being considered. N is the shape function. $\boldsymbol{K}$ the conductivity matrix. Numerical integration can therefore be used to derive the matrix form of the governing equations which can be consequently solved with iteration.

The effective diffusivity of the water vapour in different directions of the wood is often assumed to be proportional to the diffusivity of the vapour in the air, D_a, calculated as Eq. (8). [39] For this study, we assumed the effective vapour diffusivity along longitudinal, radial and tangential directions to be 98%, 5% and 8% of D_a, respectively.

$$D_a = \frac{0.026593(T/273.15)^{1.81}}{1013 + 4.615c_vT} \tag{8}$$

Diffusivity of the bound water in the transverse direction is calculate based on Eq. (9) similar to assumption of some other researchers. [33,39] Detailed parameters associated the equation is presented in Table 1. The heat transfer parameters were also similar with commonly adopted values from literature.

$$D_{bT} = D_0 exp(\frac{-E_b}{RT}) \tag{9}$$

The Bayesian updating method used in this study involves large numbers of calculation of the numerical model with randomly assigned parameters with sometimes irregular values. The numerical stability and iteration efficiency are crucial in effectiveness of

Table 1
Assumed material parameters for the finite element model.

Parameter	Model	Assumed value
ρ_0, Dry density of wood		350 kg/m^3
D_{bT}, Diffusivity for bound water in wood in the transverse direction(Frandsen [39])	$D_{bT} = D_0 \exp(\frac{-E_b}{RT})$	$D_0 = 7.0 \times 10^{-6} m/s E_b = 38500 - 29000m$m is moisture content of the wood
D_{bL}, Diffusivity for bound water in wood in the longitudinal direction(Frandsen [39])	$D_{bL} = 2.5 D_{bT}$	
EMC, Equilibrium moisture content	$EMC = k_1 H^3 + k_2 H^2 + k_3 H$	k_1 = 0.442;k_2 = -0.5964;k_3 = 0.3737; (first batch)k_1 = 0.4346;k_2 = -0.4724; k_3 = 0.3015; (second batch)
f_{lum}, Volumetric fraction of lumen(Eitelberger et al. [33])		0.4
f_{cwm}, Volumetric fraction of cell wall	$f_{cwm} = 1 - f_{lum}$	0.6
k_T, Surface heat emissivity(Eitelberger et al. [33])		*0.3 W/m^{2}K*

the method. For efficiency of the model, a simplified equation was used to calculate sorption rate from the differences between the bound water concentration and the equilibrium value, which is similar to the approach by Eitelberger et al. [33]. In their model, they use the average radius of the cell walls to build the local moisture equilibrium and calculate the sorption rate. The radius, however, often varies significantly from species to species and is unavailable to the authors for the tested wood species. [44] Also, the local equilibrium they assumed may not be reached depending on surface moisture emissivity of the cell walls. Therefore, we simply assumed that the sorption rate is related with, $D_{cwm,trans}$ diffusivity of the bound water in the transverse direction of the wood and the concentration differences of the bound water by β, a factor to be determined. Afterward, we use the Bayesian inference method to update β which contains information of the average size of the cell walls and goodness of the assumption of the local equilibrium. This equation, however, also produces a nearly linear relation and ignores differences between the rate in adsorption and desorption.

$$\dot{c} = \beta D_{cwm,trans}(c_{bl} - c_b) \tag{10}$$

We also used a simplified and monotonic sorption curve compared with the state-of-the-art model presented in Frandsen et al. [32]. The curve was a polynomial fit of the scanning curve of the hysteresis model used by Patera et al. [41] starting from the initial equilibrium state. This assumption is only solid when RH variations of the samples exposed to the climate is less significant compared with the initial drying. Also, the classic equation for equilibrium moisture content of the wood, as shown in Eq. (11), relates the moisture content with the RH. For the moisture transfer model, on the other hand, it is believed that a diffusion process based on vapour concentration is more appealing. The vapour concentration is related with RH of the air by Eq. (12) and (13).

$$EMC = k_1 H^3 + k_2 H^2 + k_3 H \tag{11}$$

$$H = \frac{c_v T}{0.002166 p_s} \tag{12}$$

$$p_s = \exp(53.421 - \frac{6516.3}{T} - 4.125\ln(T)) \tag{13}$$

Together with Eq. (11), 12 and 13, the proposed constitutive relations were implemented in the Abaqus software (ABAQUS 6.14) with a user subroutine for the user defined element (UEL). With the transfer process simplified as a 1D problem, only one layer of 10 elements was used. The initial vapour concentration, bound water and temperature assumed were listed in Table 1 together with some other modelling parameters. Together with Eq. (11), 12 and 13, the proposed constitutive relations were implemented in the Abaqus software [45] with a user subroutine for the user defined element (UEL). The UEL subroutine passes the software Jacobian matrix and residual vector of the element defined by the users, which are afterward accumulated and solved by the software. We developed the element based on Eq. (5), 6 and 7 for a three-dimensional 8-node brick element. The element has 24 degrees of freedoms with 3 variables at each node which are the water vapour concentration, bound water concentration and temperature. The moisture transfer process, however, was simplified to a 1-dimensional problem using the symmetricity. Only a line of elements was used which composed of 10 elements. One edge of the model was assumed to be isolated in terms of the thermal and mass transfer. The other edge allows heat and vapour flux calculated by Eq. (4). The surface heat and vapour flux were applied to the end element of the model based on gradient of the temperature and water vapour concentration, as shown in Eq. (14).

Using the proposed method and reported parameters in literature, moisture transfer processes were investigated regarding the tests presented by Eitelberger et al. [33] and Wadso [46]. Fig. 1 and Fig. 2 summarize the reported and presented results. As shown in the figure, the calculated results generally agree with the presented result. For the profile presented by Wadso [46] which the moisture transfer was in the radial and tangential direction, good agreement was found. For the moisture profile corresponding to longitudinal direction presented by Eitelberger et al. [33], on the other hand, larger error was found. The reason behind the error may be that the moisture profile in the longitudinal direction was mainly controlled by the sorption rate as vapour diffusivity in the longitudinal direction is much higher. The presented model, on the other hand, assumed linear sorption rate which causes error, especially when the moisture content is close to the equilibrium value. Compared with results reported by other researchers

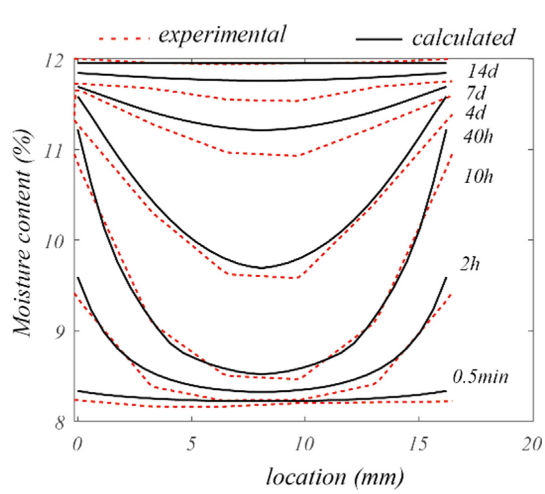

Fig. 1. Comparisons of the calculated MC profile with the experimental results presented in Wadso [46].

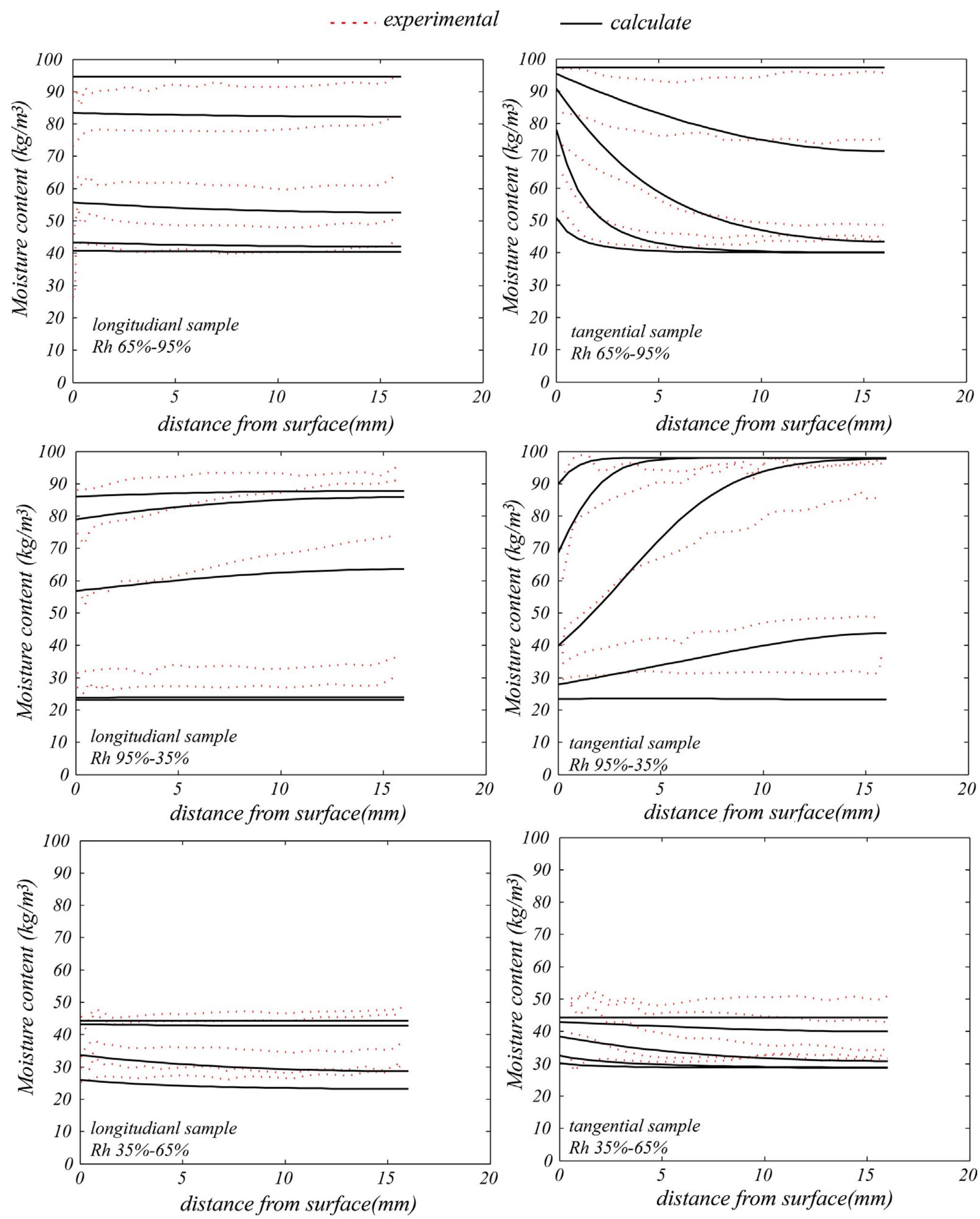

Fig. 2. Comparisons of the calculated MC profile with the experimental results presented in Eitelberger et al. [33]

using similar assumption [33], accuracy of the proposed method is believed to be acceptable.

Bayesian inference

Transport of the vapour concentration, bound water concentration and temperature in the unsteady moisture transfer process are interdependent. In addition, diffusivity of both the vapour and the bound water is strongly related with their concentration and the temperature, which makes solving the surface emissivity factor from observation of the moisture content of the wood an ill-posed inverse problem. For this kind of problem, the Bayesian inference is a robust method [36,47–49]. The Bayesian inference is based on the Bayes' theorem which can be written as:

$$p(\theta|D) = \frac{p(D|\theta)p(\theta)}{p(D)} = \frac{1}{c}p(D|\theta)p(\theta) \tag{14}$$

the equation, θ is the uncertain parameters to be determined. D is the relevant observation data corresponding to the random variables. $p(\theta|D)$ is called the posterior probability density function (PPDF), which contains information about the interested parameter set θ updated by the observation data D. $p(D|\theta)$is the likelihood function which expresses the probability of obtaining dataset D based on parameter set θ. $p(\theta)$is the prior probability density function (prior PDF) which contains the initial plausibility about distribution of θ. $p(D) = c$ is a normalizing constant guaranteeing the PPDF integrates to one and does not need to be solved in the calculation . As the equation shows, the posterior PDF of θ is proportional to the product of the probability of obtaining the observation data D based on the parameters and prior PDF of θ. With posterior PDF of θ, these parameters can be estimated either by its expectation or its maximum likelihood value.

The posterior PDF often has a non-standard form in which an explicit expression is unavailable. Also, the normalizing constant $c = p(D)$ is also often intractable except for special cases. Numerical simulations are therefore needed to explore the posterior state space. The most widely adopted method is the Markov chain Monte Carlo (MCMC) sampler which can generate samples from any probability distribution. The idea of the sampler is to construct a Markov chain which has a stationary distribution of the intended probability distribution. Explicit expression of the distribution is not necessary in using MCMC sampler. Instead, the distribution should be evaluated up to a normalizing constant, which is the case of the posterior PDF of θ in the Bayesian inference. The most widely used sampling algorithms associated with the MCMC method are the Metropolis-Hastings Sampler (M–H) and Gibbs Sampler. In this paper, M–H is used, which introduces the acceptance rate α and constructs a new transition probability matrix $\mathbf{Q}$.

$$\mathbf{Q} = \boldsymbol{\alpha} \otimes \mathbf{P} \tag{15}$$

Here, $\otimes$ means the multiplication of corresponding elements in the matrices.

Because the constant c has no effect on the calculation of distribution combined with MCMC, the posterior PDF is often expressed as follows.

$$p(\theta|D) \propto p(D|\theta)p(\theta) \tag{16}$$

The problem is transformed into calculating the right side of the above equation.

The prior PDF $p(\theta)$ has many forms of expression. Different prior PDF can eventually converge to the target distribution, and the difference lies in the efficiency of the algorithm. In this paper, the prior distribution is modelled as a uniform distribution model which assumes no prior information about the prior distribution.

$$p(\theta) = \prod_i p(x_i) \tag{17}$$

Where,

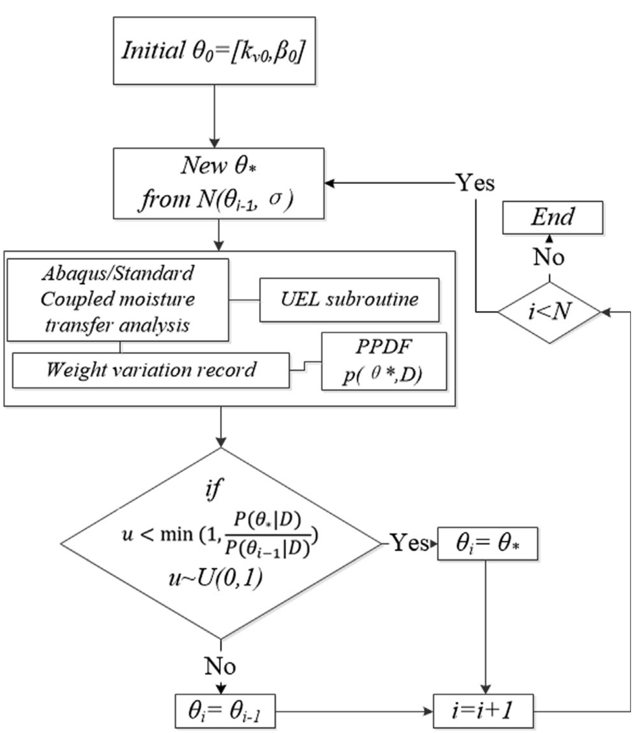

Fig. 3. Flowchart for the proposed approach.

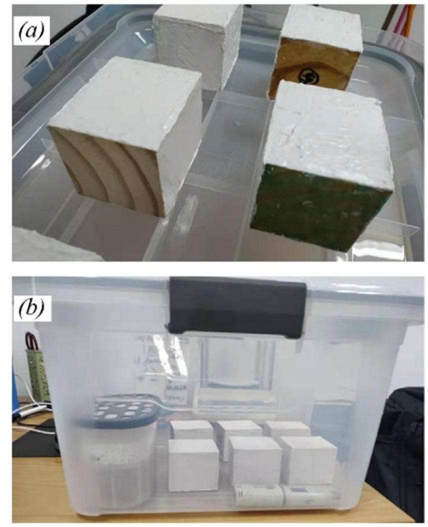

Fig. 4. Samples for measuring surface emissivity (a) photo showing surfaces of the samples (b) drying of the samples to create initial condition.

$$p(x_i) = \begin{cases} \frac{1}{b_i - a_i} & a_i \le x_i \le b_i \\ 0 & Otherwise \end{cases}$$

The likelihood function $p(D|\theta)$ is a conditional probability density function and reflects the fitting degree between the unknown model parameters and the actual observation data. The likelihood information of the unknown random variables under all observation data is included in the likelihood function. Likelihood function directly affects the efficiency of Bayesian method and also plays a key role in the accuracy and stability of the results. It is closely related to measurement error. The measurement error and the observation data are generally considered to be independent of each other. If the measurement noise is represented by ω_m, the statistical model can be expressed as follows:

$$D = F(\theta) + \omega_m \tag{18}$$

where, D denotes the data set, F is a solving operator of the positive problem. Random noise is usually modelled as stationary white noise with Gaussian distribution, so the likelihood function can be expressed as

$$p(D|\theta) = \frac{1}{(2\pi)^{n/2} {v_T}^{n/2}} exp\left(-\frac{(F(\theta) - D)^T \cdot (F(\theta) - D)}{2v_T} \right) \tag{19}$$

where, v_T is the variance. In addition, if the measurement data is abnormal, Laplace distribution can be used. The Laplace distribution can ensure the stability of the calculation process. When the measurement error can be ignored, the likelihood function can also be represented by the Dirac function.

Therefore, posterior PDF can be described as

$$p(\theta|D) \propto \frac{1}{(2\pi)^{n/2} {v_T}^{n/2}} exp\left(-\frac{(F(\theta) - D)^T \cdot (F(\theta) - D)}{2v_T} \right) \frac{1}{b_i - a_i} \tag{20}$$

It can be simplified as

$$p(\theta|D) \propto exp\left(-\frac{(F(\theta) - D)^T \cdot (F(\theta) - D)}{2v_T} \right) \tag{21}$$

In this paper, the calculated bound water concentration was subsequently integrated over length of the model and compared with weight measurement of the sample. Therefore, the solving operator F is related to the surface emissivity factor k_v and β. Thus, the posterior PDF $p(\theta|D)$ can be calculated as

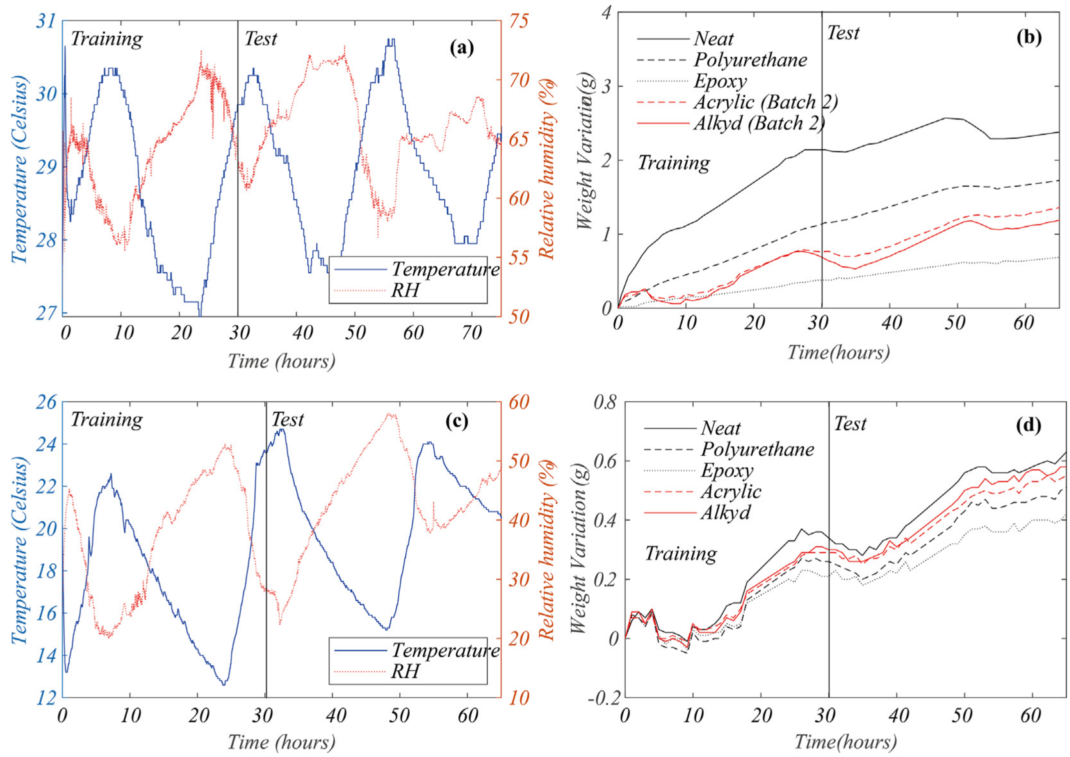

Fig. 5. (a) Variation of the ambient temperature and relative humidity for the first batch of test (b) variation of the weight of the longitudinal samples (c) variation of the ambient temperature and relative humidity for the second batch of test (d) variation of the weight of the radial samples.

$$p(\theta|D) \propto exp\left(-\frac{(F(k_v,\beta)-D)^T \cdot (F(k_v,\beta)-D)}{2\sigma^2}\right) \tag{22}$$

In which σ is standard deviation of the weight measurement. A metropolis-hasting algorithm was employed to explore the posterior distribution of k_v and β. Steps of the proposed method is summarized in Fig. 3.

3. Results and discussions

Tests were performed to validate the proposed method. Small cuboid timber samples were made from *Pinus Armandii* (Chinese white pine) wood with a dimension of 50*50*60 mm. (Fig. 4) Apart from two interested opposite square surfaces, all the other surfaces of the sample were covered with a silicone coating with 500 g/m^2 to prevent the moisture transfer. The coating was aimed to make the transfer process a 1-dimension problem to improve the computational efficiency. Samples were made separately to measure the surfaces perpendicular to the longitudinal and radial direction of the wood. Influences of different surface treatments were also investigated including the neat wood surface, wood surface covered by a polyurethane coating with a weight of 200 g/m^2, surface with epoxy coating (200 g/m^2), surface with an acrylic acid wood painting [51] of 200 g/m^2 and surface with an alkyd resin wood painting of 200 g/m^2. Altogether surface emissivity of 10 types of wood surfaces were measured. The samples were exposed to the ambient environment from an exposed corridor of an office building. The ambient RH and temperature were recorded by a small data logger. (Fig. 5) For validation purpose, the airflow rate was also recorded which were never higher than 0.3 m/s (Fig. 6). The

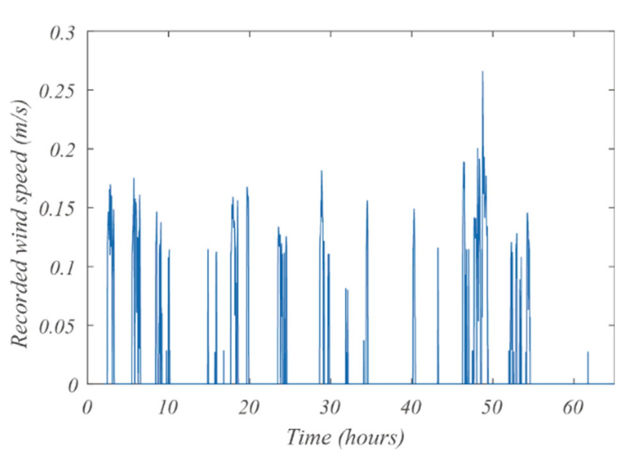

Fig. 6. Wind speed recorded during the test.

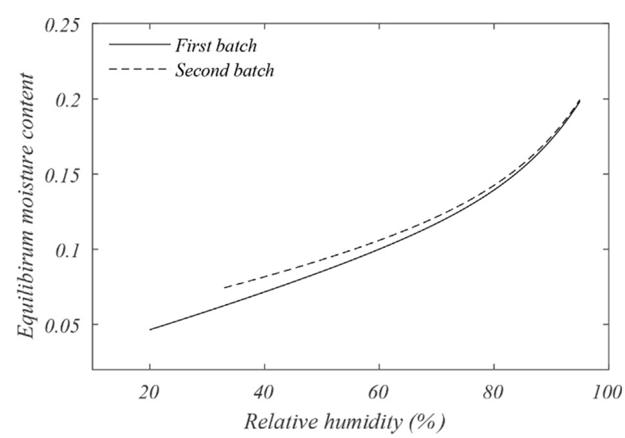

Fig. 7. Relation between the relative humidity and the equilibrium moisture content.

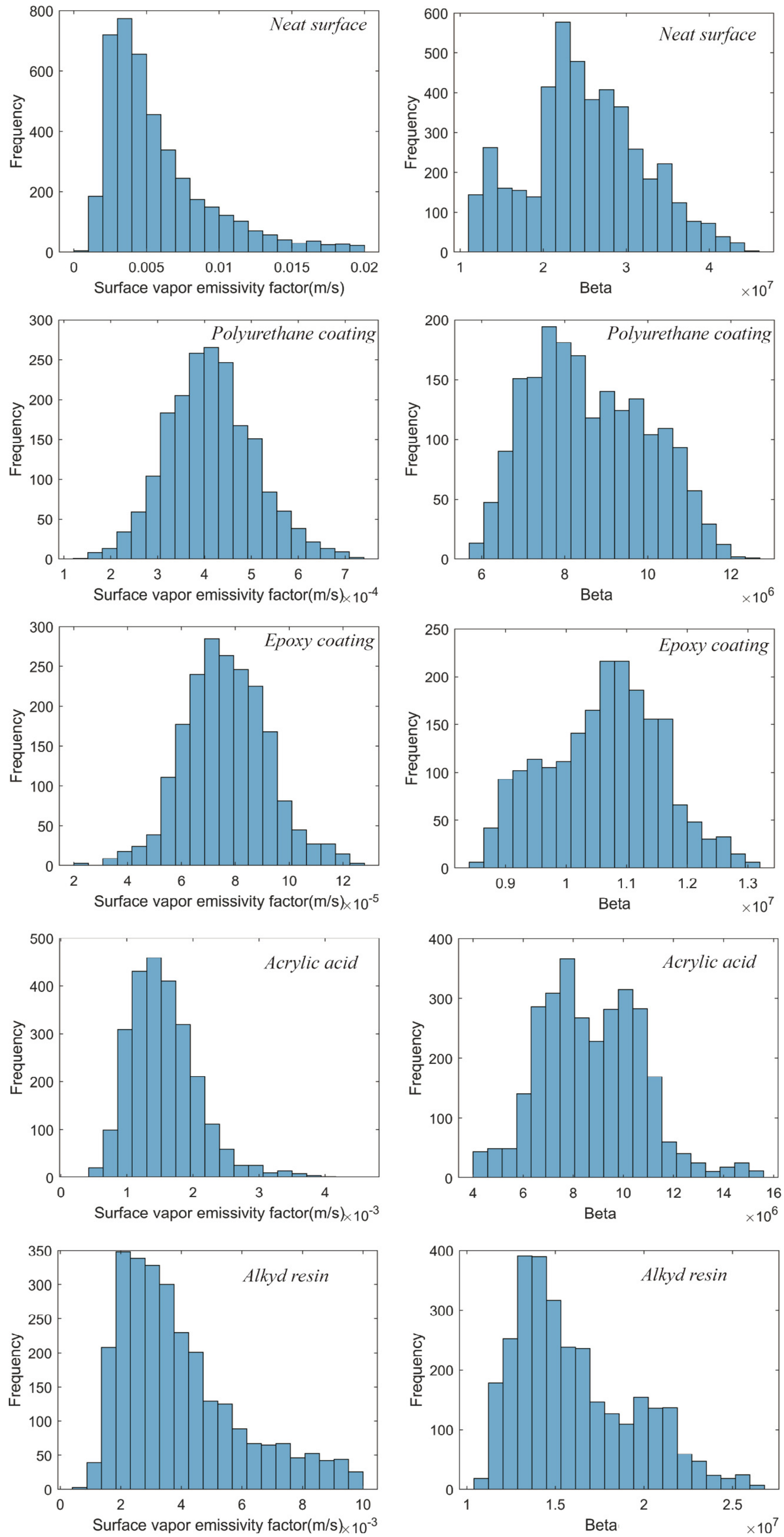

Fig. 8. Calculated distribution of k_v and β for the longitudinal samples.

weights of the samples were constantly measured by an electronic balance with an accuracy of 0.001 g. Fig. 5 shows curves of measured RH, temperature and weight variation of the samples. Two batches of samples were tested.

Prior to testing of the samples, they were stored in sealed box with silica gel desiccant for 21 days for them to reach internal moisture equilibrium. At beginning of the test, the first batch of samples has a moisture content of 4.6% while the second batch

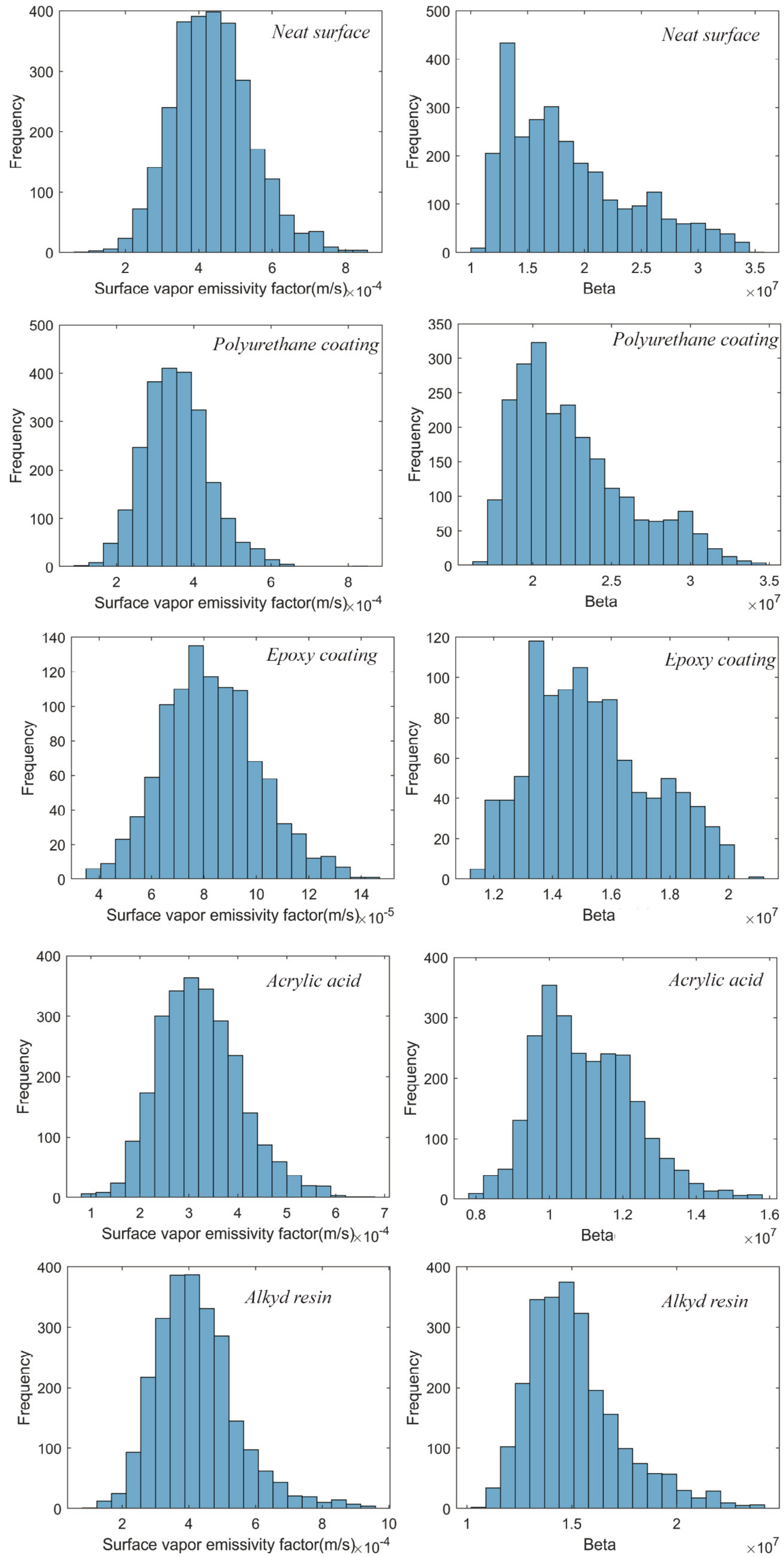

Fig. 9. Calculated distribution of k_v and β for the radial samples.

has a moisture content of 7.5%. Fig. 7 compares the sorption curves used for these two batches of samples. Using these values as the initial condition and the RH and temperature record as the boundary condition, the moisture transfer process was calculated and compared with record of the mass variations of the samples. Parameters used for the tests are summarized in Table 1.

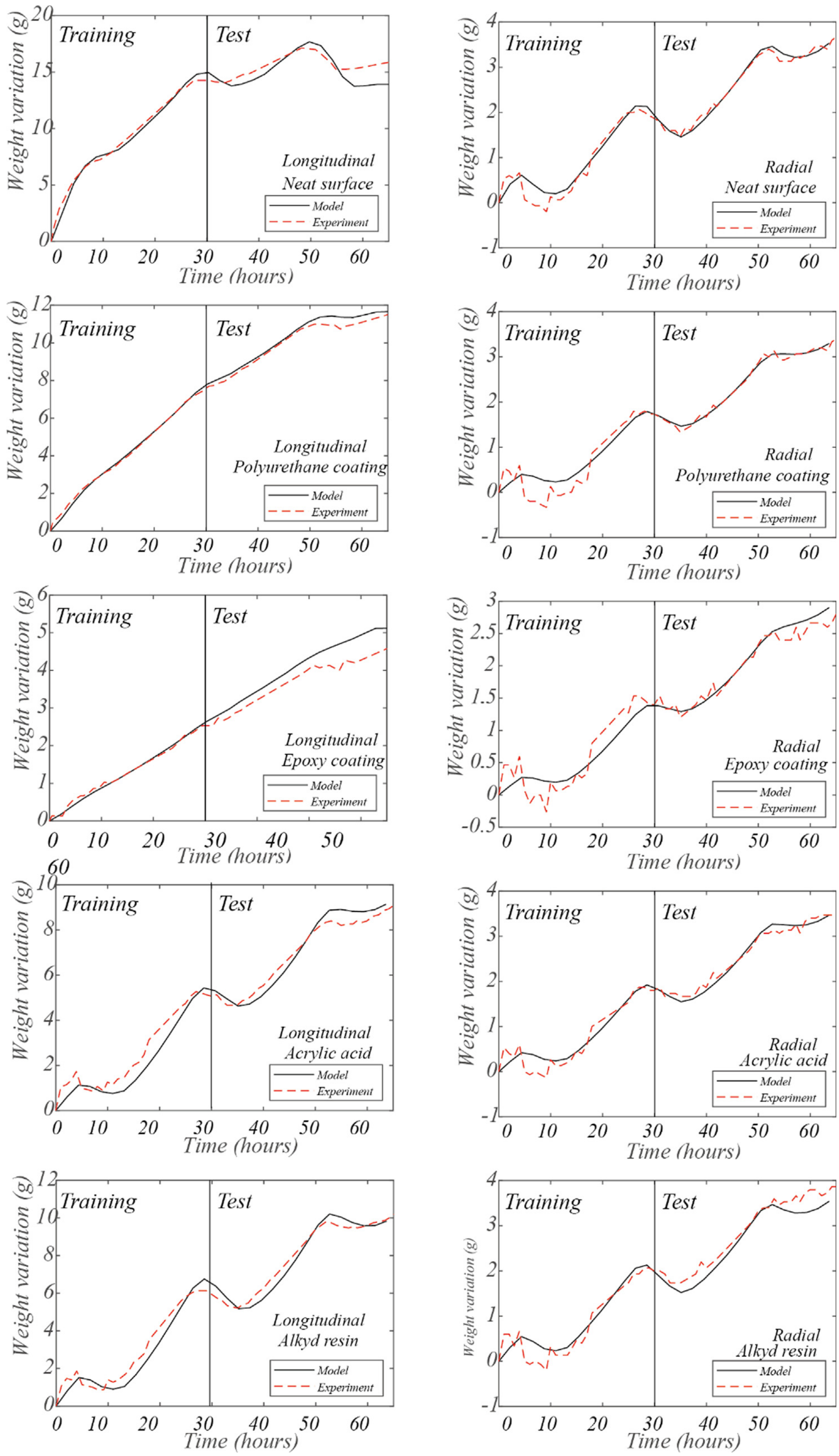

Fig. 10. Validation of the identified parameters.

Table 2
Calculated vapor emissivity and permeance factor for samples with different surface treatment.

	Longitudinal direction					Radial direction				
	Neat	PU	Epoxy	Acrylic	Alkyd	Neat	PU	Epoxy	Acrylic	Alkyd
Emissivity factor $10^{-5} m/s$	35.4	3.8	0.7	14.8	21.5	4.3	3.1	0.9	3.3	3.9
Permeance*, total 10^{-9} kg/m^2sPa	25.4	2.8	0.5	10.8	15.6	3.2	2.3	0.6	2.4	2.8
Permeance, paint 10^{-9} kg/m^2sPa	–	3.1	0.5	18.6	36.3	–	8.3	0.8	9.6	26.6

* calculated assuming a temperature of *278 K*.

Table 3
Vapor permeance adopted by different researchers in literature.

	Permeance, 10^{-9} kg/m^2sPa		
	Bergeet al. [30]	Häglund[50]	Fragiacomo et al. [17]
Neat surface		0.72	5
Alkyd oil paint	0.2–0.4	0.097–0.29	0.3
Acrylate oil paint	0.37–1.43	0.36–1.45	1
Weak paint(lime or silicate)	1–5		4
Epoxy paints	0.02–0.025		
Polyurethane varnishes	0.02		

3.1. Calculated results

Using a MCMC of 8000 iterations, k_v and β was identified for the samples. Fig. 8 and Fig. 9 summarize the calculated distribution of k_v and β for the samples with different types of coating after stability of the MCMC method. As the figure shows, these factors can be identified with good accuracy. The coefficient of variation of the calculated ratio was around 22% for k_v and 15% for β. The moisture emissivity with different types of surfaces significantly differs. For the tested samples, the emissivity factor was around 3.5×10^{-3}m/s for the neat surface perpendicular to the longitudinal direction compared with 4.3×10^{-4}m/s for that of the surface perpendicular to the radial direction. The existence of the polyurethane and epoxy coating significantly increased the surface moisture resistance of the surfaces perpendicular to the longitudinal direction. For the longitudinal samples with polyurethane coating, the surface emissivity factor was around 3.8×10^{-4}m/s compared with the emissivity factor of 7.2×10^{-5}m/s for the surface with epoxy coating. The significant reduction is probably due to sealant of the micro pores in surface of the wood, which deters exchange of vapour and air between lumen of the samples with the surrounding air. For the acrylic acid and acrylic acid painting of the same weight, on the other hand, reduction of the emissivity factor was less with an estimated surface emissivity factor of 1.5×10^{-3}m/s for the surface with acrylic acid painting and 2.15×10^{-3}m/s for the alkyd resin painting. For the wood surfaces perpendicular to the radial direction, reduction of the moisture emissivity factor with surface coating was also less. For the surfaces with polyurethane coating, the epoxy coating, the acrylic acid painting and the alkyd resin painting, the estimated moisture emissivity factors were 3.1×10^{-4}m/s, 8.2×10^{-5}m/s, 3.3×10^{-4}m/s and 3.9×10^{-4}m/s, respectively. This is understandable, as vapour travels in the radial direction of the wood much slower than that of the longitudinal direction obstructed by the cell walls. An additional layer of coating and sealant of surface pits may not be as significant. The calculated β ranges from 7.2×10^6 to $4.3 \times 10^7 kg/m^5$. At this range, variation of β were found to have limited influences on weight variation of the models.

Table 2 summarizes the calculated vapor emissivity factor based on the proposed method. Also, the permeance factors were calculated which is another parameter commonly used by researchers to qualify the surface flux based on the vapour emissivity factor assuming a temperature of 293.15 K. Permeability of the neat timber surface and the coating was separated from the painting layer by the assumption that the total moisture resistance was a sum of these two values. [13,17,30] Also, the assumed results by different researchers were summarized in Table 3 for comparison. As the table shows, the calculated results are significantly larger than the literature value, indicating a larger surface vapour flux and less resistance of the painting. The differences are probably related with environment and setup of the test. Our test was performed in open environment which introduces higher velocity in surface of the samples. Also, spread of the painting was not as even as the laboratory test and penetration was found between the painting and the wood. As research [17,50] indicates that a larger emissivity factor could lead to higher eigenstress and mechano-sorptive creep strain. The results indicate that the existing conclusions on durability of wood may need further validation for different local working environments.

3.2. Validation of the calculated surface emissivity factor

Using the identified parameter with the maximum likelihood, weight variations of the samples were subsequently calculated based on the RH and temperature record and compared with the latter portion of weight variation record. Fig. 10 compares the calculated and experimental results. As the figure shows, the calculated weight variation curve approximates the experimental results closely, both for the part of the curve used for training (identifying the surface emissivity factor) and the latter part. Slightly larger error was found at the initial part when the ambient relative humidity significantly varies. This is probably due to that the model assumed a constant sorption rate which has larger error when moisture content of the wood was closer with the equilibrium [31]. Compared with the differences caused by the surface coating in the moisture transfer process, however, these errors are much smaller.

4. Conclusions

This paper proposes a method to calculate the surface emissivity factor of timber members based on Bayesian model updating. The factor controls the moisture exchange of the wood with the surrounding air and is critical in evaluating durability and structural performance of timber members. The method only requires input of the overall weight of the samples and record of the ambient relative humidity and temperature, which makes it well suited for field measurement of the factor in different working environments. Tests were performed for demonstration and validation of the proposed method. The main conclusions of the paper are summarized as the following:

1. With sophisticated numerical model considering the coupled vapour and bound water transfer, the heat transfer and the sorption hysteresis of the wood, surface emissivity factor can be back-calculated from the variation of the overall weight of wood. The proposed method which was based on Bayesian model updating can identify the surface emissivity factor and average sorption rate of the wood samples with good accuracy.

2. Using the proposed method, moisture emissivity was measured for timber members with different kinds of surface treatment. The results show significant differences in the surface moisture emissivity of wood surfaces perpendicular to the grain and along the grain. For neat wood surface perpendicular to the longitudinal direction, the moisture emissivity factor was around 3.5×10^{-3}m/s compared with 4.3×10^{-4}m/s for the surface perpendicular to the radial direction of the wood. When surface painting and coating were applied, the emissivity factor can be further reduced to around 7.2×10^{-5}m/s. Moisture emissivity factor were measured and presented for timber surfaces with different kinds of commonly used painting and coatings.

CRediT authorship contribution statement

Zhongwen Zhang: Conceptualization, Methodology, Software. **Zhili He:** Data curation, Software, Investigation. **Zhao-Dong Xu:** Data curation, Software, Investigation. **Li-Wei Chen:** Resources, Investigation, Visualization.

Declaration of Competing Interest

The authors declare that they have no known competing financial interests or personal relationships that could have appeared to influence the work reported in this paper.

Acknowledgements

This work was financially supported by Natural Science Foundation of Jiangsu Province (BK20190365), National Science Fund for Distinguished Young Scholars (51625803) and Program of Chang Jiang Scholars of Ministry of Education. The authors wish to express their gratitude for these financial supports.

References

[1] Gereke, T. Moisture-induced stresses in cross-laminated wood panels (Doctoral dissertation, ETH Zurich), 2009.
[2] J. Jönsson, Internal stresses in the cross-grain direction in glulam induced by climate variations, Holzforschung 58 (2) (2004) 154–159.
[3] V. Angst-Nicollier, Moisture Induced Stresses in Glulam. Effect of cross section geometry and screw reinforcement. Doctoral Thesis, NTNU Trondheim, 2012.
[4] S. Svensson, G. Turk, T. Hozjan, Predicting moisture state of timber members in a continuously varying climate, Eng. Struct. 33 (2011) 3064–3070.
[5] T. Toratti, S. Svensson, Mechano-sorptive experiments perpendicular to grain under tensile and compressive loads, Wood Sci. Technol. 34 (4) (2000) 317–326.
[6] EN 1995-1-1. Eurocode 5: Design of timber structures–Part 1.1: General rules and rules for buildings, CEN, Brussels; 2004.
[7] J.A. Hingston, C.D. Collins, R.J. Murphy, J.N. Lester, Leaching of chromated copper arsenate wood preservatives: a review, Environ. Pollut. 111 (1) (2001) 53–66.
[8] D.N. Obanda, T.F. Shupe, H.M. Barnes, Reducing leaching of boron-based wood preservatives–A review of research, Bioresour. Technol. 99 (15) (2008) 7312–7322.
[9] C. Brischke, L. Meyer-Veltrup, Modelling timber decay caused by brown rot fungi, Mater. Struct. 49 (2016) 3281–3291.
[10] J.H. Jönsson, Internal stresses in glulam due to moisture gradients in the grain direction, Holzforschung 59 (1) (2005) 18–22.
[11] V. Angst, K.A. Malo, Moisture induced stresses perpendicular to the grain in glulam: review and evaluation of the relative importance of models and parameters, Holzforschung 64 (5) (2010) 609–617.
[12] V. Angst, K.A. Malo, The effect of climate variations on glulam—an experimental study, Eur. J. Wood Wood Prod. 70 (5) (2012) 603–613.
[13] S. Fortino, P. Hradil, A. Genoese, A. Genoese, A. Pousette, Numerical hygro-thermal analysis of coated wooden bridge members exposed to Northern European climates, Constr. Build. Mater. 208 (2019) 492–505.
[14] D. Konopka, M. Kaliske, Transient multi-Fickian hygro-mechanical analysis of wood, Comput. Struct. 197 (2018) 12–27.
[15] T. Gereke, P. Niemz, Moisture-induced stresses in spruce cross-laminates, Eng. Struct. 32 (2) (2010) 600–606.
[16] E.V. Bachtiar, D. Konopka, B. Schmidt, P. Niemz, M. Kaliske, Hygro-mechanical analysis of wood-adhesive joints, Eng. Struct. 193 (2019) 258–270.
[17] M. Fragiacomo, S. Fortino, D. Tononi, I. Usardi, T. Toratti, Moisture-induced stresses perpendicular to grain in cross-sections of timber members exposed to different climates, Eng. Struct. 33 (11) (2011) 3071–3078.
[18] S. Fortino, A. Genoese, A. Genoese, L. Nunes, P. Palma, Numerical modelling of the hygro-thermal response of timber bridges during their service life: a monitoring case-study, Constr. Build. Mater. 47 (2013) 1225–1234.
[19] V. Angst, K.A. Malo, Moisture-induced stresses in glulam cross sections during wetting exposures, Wood Sci. Technol. 47 (2) (2013) 227–241.
[20] M.P. Rostand, F. Dubois, N. Sauvat, E. Fournely, Strain analysis in dried green wood: Experimentation and modelling approaches, Eng. Fract. Mech. 105 (2013) 182–199.
[21] F. Thuvander, L. Wallström, L.A. Berglund, K.A.H. Lindberg, Effects of an impregnation procedure for prevention of wood cell wall damage due to drying, Wood Sci. Technol. 34 (6) (2001) 473–480.
[22] J.G. Salin, Problems and solutions in wood drying modelling: History and future, Wood Mat. Sci. Eng. 5 (2) (2010) 123–134.
[23] E.T. Choong, C. Skaar, Diffusivity and surface emissivity in wood drying, Wood Fiber Sci. 4 (2) (2007) 80–86.
[24] J.F. Siau, S. Avramidis, The surface emission coefficient of wood, Wood Fiber Sci. 28 (2) (2007) 178–185.
[25] J.Y. Liu, W.T. Simpson, Solutions of diffusion equation with constant diffusion and surface emission coefficients, Drying Technol. 15 (10) (1997) 2459–2477.
[26] P. Koc, M. Houška, Characterization of the sorptive properties of spruce wood by the Inverse Identification Method, Eur. J. Wood Wood Prod. 60 (4) (2002) 265–270.
[27] H. Yeo, W.B. Smith, Development of a convective mass transfer coefficient conversion method, Wood Fiber Sci. 37 (1) (2007) 3–13.
[28] K. Krabbenhøft, Moisture Transport in Wood. A Study of Physical-Mathematical Models and their Numerical Implementation Ph.D. Thesis, Department of Civil Engineering Technical University of Denmark, 2003.
[29] J.F. Siau, S. Avramidis, Application of a thermodynamic model to experiments on nonisothermal diffusion of moisture in wood, Wood Sci. Technol. 27 (2) (1993) 131–136.
[30] B. Berge, The Ecology of Building Materials, Second Edition., Architectural Press, Elsevier, 2009.
[31] K. Krabbenhøft, L. Damkilde, A model for non-Fickian moisture transfer in wood, Mater. Struct. 37 (9) (2004) 615–622.
[32] H.L. Frandsen, L. Damkilde, S. Svensson, A revised multi-Fickian moisture transport model to describe non-Fickian effects in wood, Holzforschung 61 (5) (2007) 563–572.
[33] J. Eitelberger, K. Hofstetter, S.V. Dvinskikh, A multi-scale approach for simulation of transient moisture transport processes in wood below the fiber saturation point, Compos. Sci. Technol. 71 (15) (2011) 1727–1738.
[34] J.F. Siau, Transport processes in wood, Vol. 2, Springer Science & Business Media, 2012.
[35] J. Wang, N. Zabaras, A Bayesian inference approach to the inverse heat conduction problem, Int. J. Heat Mass Transf. 47 (17–18) (2004) 3927–3941.
[36] S. Parthasarathy, C. Balaji, Estimation of parameters in multi-mode heat transfer problems using Bayesian inference–Effect of noise and a priori, Int. J. Heat Mass Transf. 51 (9–10) (2008) 2313–2334.
[37] Z. Cai, A new method of determining moisture gradient in wood, Forest Products J. 58 (2008) 41–45.
[38] P. Pourmand, L. Wang, S.V. Dvinskikh, Assessment of moisture protective properties of wood coatings by a portable NMR sensor, J. Coat. Technol. Res. 8 (5) (2011) 649–654.
[39] H.L. Frandsen, Modelling of Moisture Transport in Wood: State of the Art and Analytic Discussion.Aalborg University. Wood Science and Timber Engineering, No. Paper 1, Aalborg Universitet. Instituttet for Bygningsteknik. R, No. R502, 2005.
[40] P.N. Peralta, A.P. Bangi, Modeling wood moisture sorption hysteresis based on similarity hypothesis. Part II. Capillary-radii approach. Wood and fiber science: Journal of the Society of, Wood Sci. Technol. 30 (2) (1998) 148–154.
[41] A. Patera, H. Derluyn, D. Derome, J. Carmeliet, Influence of sorption hysteresis on moisture transport in wood, Wood Sci. Technol. 50 (2) (2016) 259–283.
[42] P.N. Peralta, Sorption of moisture by wood within a limited range of relative humidities, Wood Fiber Sci. 27 (1) (2007) 13–21.
[43] C.R. Pedersen, Combined heat and moisture transfer in building constructions (Vol. 214). Thermal Insulation Laboratory, Technical University of Denmark, 1990.
[44] M. Plötze, P. Niemz, Porosity and pore size distribution of different wood types as determined by mercury intrusion porosimetry, Eur. J. Wood Wood Prod. 69 (4) (2011) 649–657.
[45] ABAQUS User's Guide and Theoretical Manual. "Version 6.14, Hibbit, Karlson, and Sorenson." Inc.: Pawtucket, RI; 2014.
[46] L. Wadso, Surface mass transfer coefficients for wood, Drying Technol. 11 (6) (1993) 1227–1249.
[47] J.P. Kaipio, C. Fox, The Bayesian framework for inverse problems in heat transfer, Heat Transfer Eng. 32 (9) (2011) 718–753.
[48] B. Goller, G.I. Schueller, Investigation of model uncertainties in Bayesian structural model updating, J. Sound Vib. 330 (25) (2011) 6122–6136.
[49] J. Cao, H. Xiong, J. Chen, A. Huynh, Bayesian parameter identification for empirical model of CLT connections, Constr. Build. Mater. 218 (2019) 254–269.
[50] M. Häglund, Parameter influence on moisture induced eigen-stresses in timbers, Eur. J. Wood Wood Prod. 68 (4) (2010) 397–406.
[51] Zhao-Dong Xu, Teng Ge, Jie Liu, Experimental and theoretical study of high energy dissipation viscoelastic dampers based on acrylate rubber matrix, Journal of Engineering Mechanics, ASCE 146 (6) (2020) 04020057, https://doi.org/10.1061/(ASCE)EM.1943-7889.0001802.